Ionization Above the Coulomb Barrier

Armin Scrinzi, Michael Geissler, and Thomas Brabec*
Institut für Angewandte Elektronik und Quantenelektronik, Vienna University of Technology, Gusshausstrasse 27-29, A-1040 Vienna, Austria
(Received 24 July 1998)

The interaction of noble gases with laser pulses in the near-infrared and visible wavelength regime is dominated by above barrier ionization while tunnel ionization plays a subordinate role. We develop a theory of ionization in this parameter range. A condition for the applicability of the quasistatic approximation in the above barrier ionization regime is obtained. Ionization of arbitrary atoms by a laser pulse may then be calculated from static ionization rates. The static ionization rate of He is obtained by solving the full two-electron Schrödinger equation. Our analysis yields a verification of the single active electron approximation and indicates the possibility to create keV radiation by high harmonic generation in a He gas.

PACS numbers: 32.80.Rm, 32.80.Fb

When matter is exposed to high intensity laser fields, a wealth of exciting phenomena can be observed including high harmonic generation (HHG) [1], above threshold ionization [2], atomic stabilization [3], x-ray lasing [4], laser-induced damage of dielectrics [5], molecular dissociation [6], etc. The key process triggering all of these strong field phenomena is ionization.

The theoretical investigation of the above processes is significantly simplified by the analytical description of ionization. This has been achieved in two parameter ranges defined by $\gamma \gg 1$ and $\gamma \ll 1$, where γ is the Keldysh parameter [7]. For $\gamma \gg 1$, ionization is weak and can be described as a perturbative multiphoton process. Tunnel ionization, which takes place in the opposite limit $\gamma \ll 1$, is modeled by the Ammosov-Delone-Krainov (ADK) theory [8]. The power of the ADK theory lies in the fact that the quasistatic approximation (QSA) applies in the tunneling regime. As a result, dynamic ionization processes may be evaluated by the use of closed-form static field ionization rates.

A third ionization regime, termed above barrier ionization (ABI), exists for field strengths $E > E_{\mathrm{bs}}$ at which the barrier of the Coulomb potential becomes suppressed by the electric field [9] and the electron escapes directly from the potential well without tunneling. A simple estimation given below shows that the Keldysh parameter γ_{bs} corresponding to E_{bs} for noble gases and for laser wavelengths in the visible and near infrared is $\gamma_{\mathrm{bs}} \approx 1$. That means that in the near infrared and visible wavelength range multiphoton ionization goes over directly into ABI and tunnel ionization plays only a minor role. Consequently, the static ADK ionization rates [10] and the Keldysh parameter as a measure of the validity of the QSA, which are based on the assumption of a barrier, loose their validity.

As the wavelength range below $1\,\mu$m is of central importance for strong field physics, it is indispensable to find a generalized ionization theory which covers ABI and corrects for the above mentioned deficiencies of tunneling theories. This is the purpose of the present paper. The main results of our analysis are: (i) In contrast to tunneling theory the range of validity of the QSA in the ABI regime is not determined by the Keldysh parameter, but by a critical field strength which is nearly independent of the laser center frequency. (ii) We determine the exact static ionization rates of H and He numerically by using the complex scaling technique [11,12]. The ionization rates of He are to our knowledge the first accurate results for a two electron atom. The rates for more complex atoms could be obtained by using R-matrix techniques [13]. (iii) The good agreement between the ADK rates and the exact static ionization rates of He in the tunneling regime corroborates the validity of the single active electron approximation (SAEA), which is of central importance for the numerical analysis of strong field phenomena in many electron atoms [14]. (iv) The corrected ionization dynamics has important implications for strong field phenomena. We show that the exact ionization rates are considerably smaller than predicted by the ADK theory which leads to a shift of the cutoff for HHG to shorter wavelengths. A simple analysis reveals that the cutoff for HHG with a few cycle laser pulse in He is shifted above 1 keV photon energy.

The evolution of a He atom in an electric field is determined by the two electron Hamiltonian (in atomic units)

$$H = -\frac{1}{2}(\Delta_1 + \Delta_2) - \frac{Z}{r_1} - \frac{Z}{r_2} + \frac{1}{|\mathbf{r}_1 - \mathbf{r}_2|} + \mathbf{E}(t)\cdot(\mathbf{r}_1 + \mathbf{r}_2), \tag{1}$$

where $\mathbf{r}_1$ and $\mathbf{r}_2$ denote the electron coordinates measured from the nucleus and $\mathbf{\Delta}_{1,2}$ are the respective Laplace operators. The interaction between the electrons and the electric field $\mathbf{E}$ is treated in the dipole approximation. For a He atom the nuclear charge is $Z = 2$. In the case of hydrogen the electron-electron interaction is omitted and the nuclear charge is set to $Z = 1$. The static ionization rates are calculated by using the complex scaling method, which consists in multiplying the coordinates $\mathbf{r}_i$ of the

 0031-9007/99/83(4)/706(4)$15.00

Hamiltonian (1) by a complex factor $e^{i\theta}$ [11]. The resulting non-Hermitian Hamiltonian has complex eigenvalues, whose imaginary parts give one-half of the ionization rate. This has been rigorously proven for hydrogen in static electric fields [15]. The eigenvalues are determined variationally, where for H a finite elements basis set was used. The explicitly correlated basis set for He is described in detail in Ref. [12]. The time-dependent Schrödinger equation for H is solved after transformation to velocity gauge by expansion in Laguerre polynomials, with outgoing wave boundary conditions implemented through complex scaling [12].

Our analysis starts with the investigation of ABI for H, where ionization rates can be determined numerically with very high accuracy. The rates are depicted in Fig. 1 versus the electric field strength. The full and the dashed lines denote the ionization rate as obtained by the numerical solution of Eq. (1) and the ADK ionization rate [8], respectively. The dotted line marks the field strength $E_{\mathrm{bs}} = I_{\mathrm{p}}^2/4$ at which the Coulomb barrier is suppressed with I_{p} the atomic ionization potential. For electric fields $E < E_{\mathrm{bs}}$ the ADK rate approaches the numerical data to within 20%. For field strengths above E_{bs} the ADK rate strongly overestimates the actual ionization rate.

The central importance of the ADK theory is due to the fact that, in combination with the QSA, ionization yields for time-dependent laser fields can be calculated by

$$\frac{n(t)}{n_0} = 1 - \exp\left[-\int_{-\infty}^{t} dt'\, w(E(t'))\right], \qquad (2)$$

where $n(t)$ is the density of free electrons, n_0 is the initial gas density, and w is the static field ionization rate. In tunneling theories [7] the validity of the QSA is determined by $\gamma \ll 1$, where the Keldysh parameter $\gamma = \sqrt{2I_p}\,\omega_0/E$ is defined as the ratio of the tunneling time and the inverse center frequency of the laser pulse, $1/\omega_0$. Here, E is the peak electric field strength of the laser pulse. According to the Keldysh condition the QSA applies as long as the electric field may be regarded constant during the tunneling time.

ABI occurs for electric field strengths $E \geq E_{\mathrm{bs}}$. Inserting E_{bs} into the Keldysh parameter yields $\gamma_{\mathrm{bs}} = 16\omega_0/(2I_p)^{3/2}$. In strong field experiments preferably noble gases (Kr, Ar, Ne, He) are used because of their chemical inactivity, the ground state ionization potentials of which range between 0.5 and 0.9 a.u. For noble gases exposed to low frequency radiation, such as a CO_2 laser with a center wavelength $\lambda_0 = 10\ \mu\mathrm{m}$ ($\omega_0 = 0.004\,56$ a.u.), the Keldysh parameter $\gamma_{\mathrm{bs}} \approx 0.05 \ll 1$. That means with increasing field strength the ionization mechanism changes from multiphoton to tunnel ionization and finally at $\gamma \approx 0.05$ into ABI. However, estimation of the Keldysh parameter in the UV to near infrared wavelength range gives $\gamma_{\mathrm{bs}} \approx 0.5$–$2$. In contrast to a low frequency radiation field for which tunnel ionization is dominant, in the visible and near infrared frequency range multiphoton ionization goes over directly into ABI and tunnel ionization plays only a minor role. Therefore, the tunneling time is no longer a meaningful measure of the time required for the electron to be set free, and the use of the Keldysh parameter as a measure for the validity of the QSA becomes questionable.

To identify the range of validity of the QSA in the ABI regime, we have calculated the fraction of H atoms ionized in a pulsed laser field by an exact solution of the time-dependent Schrödinger equation and by using the QSA in combination with the static field ionization rates depicted in Fig. 1. The ionization yield versus the electric field strength is plotted in Fig. 2. The vector potential of the pulse is assumed to be $A(t) = E/\omega_0\,\mathrm{sech}(t/\tau)\sin(\omega_0 t)$, where the full width at half maximum pulse duration $\tau = 206.7$ a.u. (5 fs) and $\omega_0 = 0.057$ a.u. (wavelength $\lambda_0 = 800$ nm). The full circles represent the numerical solution of Eq. (1) for the time-dependent electric field. The

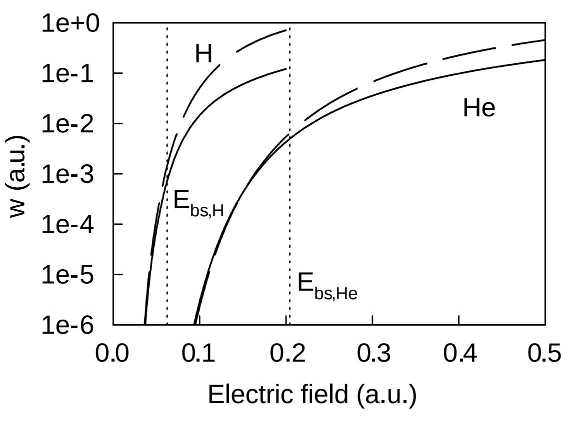

FIG. 1. Static field ionization rates of H and He versus the electric field strength in atomic units. Solid line: numerical result; dashed line: ADK formula. The dotted line denotes the barrier suppression field strength for H and He.

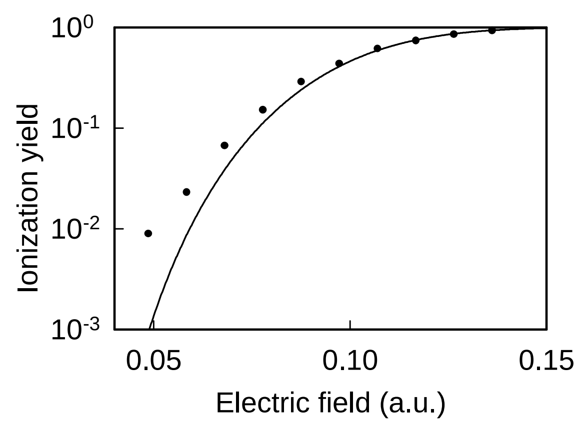

FIG. 2. Ionization yield of H versus the peak electric field strength of the laser pulse; for the pulse parameters, see the text. The full circles denote the solution of the Schrödinger equation for the laser pulse; the full line refers to the ionization yield obtained by the QSA in combination with the exact static ionization rate.

full line denotes the ionization yield as obtained by the static ionization rate. We have defined a field strength E_{qs} above which the two calculations deviate by less than 5%. For $E > E_{\mathrm{qs}}$ the QSA is applicable. From Fig. 2 we obtain $E_{\mathrm{qs}} \approx 0.1$. The same calculation was repeated for various wavelengths between 1 and 0.25 μm keeping the product $\tau\omega_0$ constant. In the whole wavelength range, we obtained a nearly constant field strength, $E_{\mathrm{qs}} \approx 0.1$. This is in contradiction to the prediction from the Keldysh parameter which implies a wavelength dependence of E_{qs}. Note that $E_{\mathrm{bs}} = 1/16 < E_{\mathrm{qs}}$ for hydrogen which shows that the Coulomb barrier is suppressed before the QSA becomes valid. Inserting E_{qs} into the Keldysh parameter gives $0.5 < \gamma_{\mathrm{qs}} < 2$ in the inspected wavelength range. Hence, the condition determining the validity of the QSA for ABI is less restrictive than the Keldysh criterion $\gamma \ll 1$ for tunnel ionization. A future challenge will be the generalization of the validity condition for the QSA to arbitrary atoms. This can be done by performing similar calculations based on the SAEA [14].

In the case of H, it was shown that the static tunneling rates are not valid in the ABI regime. Therefore, it is necessary to tabulate static field ionization rates for atoms frequently used in strong field experiments, such as the noble gases. An important task will be the calculation of these rates. To begin with, the static ionization rates obtained from the complex-scaled Hamiltonian (1) are listed in Table I. For more complex atoms, ionization rates could be calculated, e.g., by atomic R-matrix techniques that have been used for the solution of the Schrödinger equation of general atoms [13].

TABLE I. Static field ionization rates from the ground state of He in atomic units. The conversion factors to SI units are 1 (time) a.u. $= 2.419 \times 10^{-17}$ s, 1 (electric field strength) a.u. $= 5.142 \times 10^{11}$ V/m. The numerical data is accurate to at least two digits.

E	w	E	w	E	w
0.08	0.463×10^{-7}	0.28	0.266×10^{-1}	0.48	0.164
0.09	0.509×10^{-6}	0.29	0.309×10^{-1}	0.49	0.174
0.10	0.288×10^{-5}	0.30	0.356×10^{-1}	0.50	0.183
0.11	0.115×10^{-4}	0.31	0.405×10^{-1}	0.55	0.233
0.12	0.362×10^{-4}	0.32	0.458×10^{-1}	0.60	0.287
0.13	0.943×10^{-4}	0.33	0.513×10^{-1}	0.65	0.345
0.14	0.212×10^{-3}	0.34	0.572×10^{-1}	0.70	0.406
0.15	0.423×10^{-3}	0.35	0.633×10^{-1}	0.75	0.470
0.16	0.768×10^{-3}	0.36	0.696×10^{-1}	0.80	0.536
0.17	0.129×10^{-2}	0.37	0.763×10^{-1}	0.85	0.604
0.18	0.203×10^{-2}	0.38	0.832×10^{-1}	0.90	0.673
0.19	0.302×10^{-2}	0.39	0.903×10^{-1}	0.95	0.744
0.20	0.431×10^{-2}	0.40	0.977×10^{-1}	1.00	0.818
0.21	0.590×10^{-2}	0.41	0.105	1.10	0.97
0.22	0.783×10^{-2}	0.42	0.113	1.20	1.13
0.23	0.101×10^{-1}	0.43	0.121	1.30	1.29
0.24	0.127×10^{-1}	0.44	0.129	1.40	1.45
0.25	0.157×10^{-1}	0.45	0.138	1.50	1.61
0.26	0.190×10^{-1}	0.46	0.146	1.60	1.77
0.27	0.226×10^{-1}	0.47	0.155	1.70	1.92

The numerical and the ADK ionization rate of He are plotted in Fig. 1 versus the electric field strength. As for hydrogen, in the tunneling regime we find reasonable agreement between the numerical and analytical results within about 30%. This corroborates the validity of the SAEA, which is the basis for the numerical simulation of strong field phenomena in many-electron systems. In the barrier suppression regime ionization is less than predicted by the ADK theory. As a consequence, He atoms can be exposed to higher intensities than predicted by the tunneling theory before the ground state is depleted. This finding has important implications for high harmonic generation, since the harmonic cutoff is proportional to the intensity at which the ground state is depleted [16]. Therewith, the order of the cutoff harmonic depends sensitively on the ionization rate. In Fig. 3 the order of the cutoff harmonic with respect to the valence electron of He is depicted versus the pulse duration. The cutoff harmonic for a given pulse duration is determined by the saturation intensity at which 98% of the He atoms are ionized. The ionization was calculated by Eq. (2). The full and the dashed lines denote the cutoff harmonic as obtained by the numerical ionization rate of Table I and by the ADK ionization rate, respectively. The difference between the two results increases with decreasing pulse duration. For a single cycle pulse, the ADK rate underestimates the order of the cutoff harmonic by 40%. In contrast to calculations based on the ADK rates, use of the exact static ionization rates shows that the cutoff harmonic is shifted to photon energies above the "magic" 1 keV barrier. This parameter range is of great importance for a number of applications, such as time-resolved x-ray diffraction experiments [17].

In conclusion, ABI is the dominant ionization mechanism in noble gases for laser wavelengths below 1 μm,

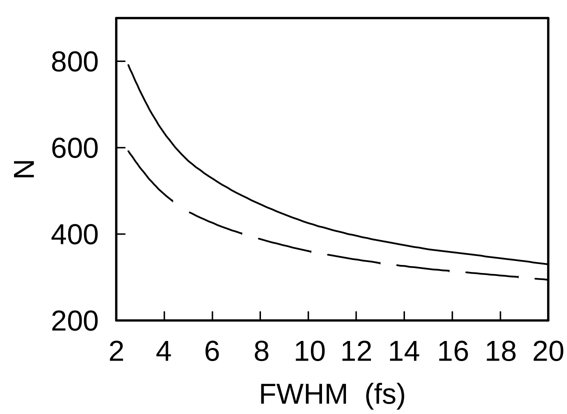

FIG. 3. Order of the cutoff harmonic in helium versus the pulse duration ($\lambda_0 = 800$ nm), as calculated by using the exact static ionization rates of Table (I) (full line) and the ADK rate (dashed line). The cutoff harmonic for a given pulse duration is determined by the saturation intensity at which 98% of the He atoms are ionized.

where tunnel ionization plays only a minor role. We extended existing tunneling theories to describe ionization properly in the ABI regime. A condition for the validity of the quasistatic approximation for ABI was established. We determined the exact static ionization rate of He by solving the full two-electron Schrödinger equation. The corrected ionization rates have important implications for HHG in helium indicating that the generation of harmonics with photon energies above 1 keV might be possible.

The authors gratefully acknowledge the support of Professor A. J. Schmidt and valuable discussions with Professor F. Krausz. This work was supported by the Austrian Fonds zur Förderung der Wissenschaftlichen Forschung, Grant No. P12631-PHY, and by the Austrian Nationalbank Jubiläumsfondsprojekt 7178.

*Electronic address: brabec@rs6.iaee.tuwien.ac.at

[1] B. Corkum, Phys. Rev. Lett. **71**, 1994 (1993); A. L'Huillier and P. Balcou, Phys. Rev. Lett. **70**, 774 (1993); J. J. Macklin *et al.*, Phys. Rev. Lett. **70**, 766 (1993).
[2] P. B. Corkum *et al.*, Phys. Rev. Lett. **62**, 1259 (1989).
[3] M. Pont and M. Gavrila, Phys. Rev. Lett. **65**, 2362 (1990); M. Pont and R. Shakeshaft, Phys. Rev. A **44**, R4110 (1991).
[4] B. E. Lemoff, C. P. J. Barty, and S. E. Harris, Opt. Lett. **19**, 569 (1994).
[5] B. C. Stuart *et al.*, Phys. Rev. Lett. **74**, 2248 (1995); D. Du *et al.*, Appl. Phys. Lett. **64**, 3071 (1994).
[6] T. Seidemann *et al.*, Phys. Rev. Lett. **75**, 2819 (1995); S. Chelkowski *et al.*, Phys. Rev. A **54**, 3235 (1996).
[7] V. Keldysh, Sov. Phys. JETP **20**, 1307 (1965); F. H. M. Faisal, J. Phys. B **6**, L89 (1973); H. R. Reiss, Phys. Rev. A **22**, 1786 (1980).
[8] A. M. Perelomov *et al.*, Sov. Phys. JETP **23**, 924 (1966); V. Ammosov *et al.*, Sov. Phys. JETP **64**, 1191 (1986).
[9] S. Augst *et al.*, Phys. Rev. Lett. **63**, 2212 (1989); S. Augst *et al.*, J. Opt. Soc. Am. B **8**, 858 (1991); V. P. Krainov, J. Opt. Soc. Am. B **14**, 425 (1997).
[10] Ch. Spielmann *et al.*, IEEE J. Sel. Top. Quantum Electron. **4**, 249 (1998).
[11] W. Reinhardt, Annu. Rev. Phys. Chem. **33**, 223 (1982).
[12] A. Scrinzi and B. Piraux, Phys. Rev. A **58**, 1310 (1998).
[13] P. G. Burke, P. Francken, and C. J. Joachain, Europhys. Lett. **13**, 617 (1990); J. Phys. B **24**, 761 (1991); P. G. Burke and V. M. Burke, J. Phys. B **30**, L383 (1997).
[14] J. L. Krause *et al.*, Phys. Rev. Lett. **68**, 3535 (1992); J. L. Krause *et al.*, Phys. Rev. A **45**, 4998 (1992).
[15] I. W. Herbst, Commun. Math. Phys. **75**, 179 (1980).
[16] Z. Chang *et al.*, Phys. Rev. Lett. **79**, 2967 (1997).
[17] C. Rischel *et al.*, Nature (London) **390**, 490 (1997).